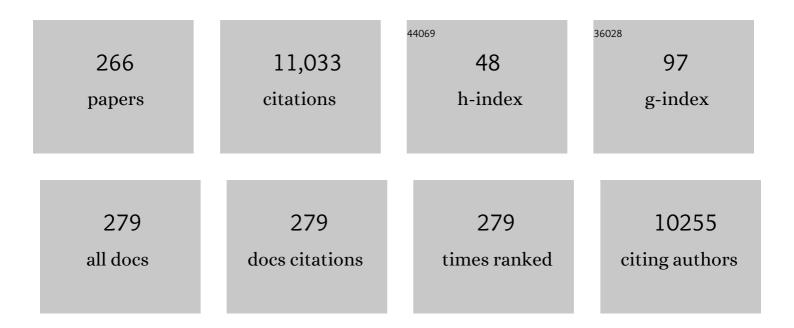
## Takao Shimizu

List of Publications by Year in descending order

Source: https://exaly.com/author-pdf/2159285/publications.pdf Version: 2024-02-01



ΤΛΚΛΟ ΟΗΙΜΙΖΗ

#	Article	IF	CITATIONS
1	Effect of Film Microstructure on Domain Nucleation and Intrinsic Switching in Ferroelectric Y:HfO <sub>2</sub> Thin Film Capacitors. Advanced Functional Materials, 2022, 32, 2108876.	14.9	23
2	Domain structures induced by tensile thermal strain in epitaxial PbTiO3 films on silicon substrates. Journal of Applied Physics, 2022, 131, 035301.	2.5	2
3	Noâ€Heating Deposition of 1â€î¼mâ€Thick Yâ€Doped HfO <sub>2</sub> Ferroelectric Films with Good Ferroelectric and Piezoelectric Properties by Radio Frequency Magnetron Sputtering Method. Physica Status Solidi - Rapid Research Letters, 2022, 16, .	2.4	2
4	Polar-axis-oriented epitaxial tetragonal (Bi,K)TiO3 films with large remanent polarization deposited below Curie temperature by a hydrothermal method. Applied Physics Letters, 2022, 120, 022903.	3.3	6
5	Lipid Profiles of Human Serum Fractions Enhanced with CD9 Antibody-Immobilized Magnetic Beads. Metabolites, 2022, 12, 230.	2.9	0
6	TRACES: A Lightweight Browser for Liquid Chromatography–Multiple Reaction Monitoring–Mass Spectrometry Chromatograms. Metabolites, 2022, 12, 354.	2.9	4
7	Preparation of orthorhombic Y-doped TaON film. Journal of the Ceramic Society of Japan, 2022, 130, 432-435.	1.1	2
8	Lattice deformation and phase transition of aluminum nitride studied by density functional theory calculations. Journal of the Ceramic Society of Japan, 2022, 130, 452-457.	1.1	2
9	Lower ferroelectric coercive field of ScGaN with equivalent remanent polarization as ScAlN. Applied Physics Express, 2022, 15, 081003.	2.4	5
10	Enhancement of crystal anisotropy and ferroelectricity by decreasing thickness in (Al,Sc)N films. Journal of the Ceramic Society of Japan, 2022, 130, 436-441.	1.1	11
11	Lamellar-like nanostructure in a relaxor ferroelectrics Pb(Mg1/3Nb2/3)O3. Journal of Materials Science, 2021, 56, 1231-1241.	3.7	7
12	Mapping membrane lipids in the developing and adult mouse retina under physiological and pathological conditions using mass spectrometry. Journal of Biological Chemistry, 2021, 296, 100303.	3.4	12
13	Electricâ€Fieldâ€Induced Ferroelectricity in 5%Yâ€doped Hf <sub>0.5</sub> Zr <sub>0.5</sub> O <sub>2</sub> : Transformation from the Paraelectric Tetragonal Phase to the Ferroelectric Orthorhombic Phase. Physica Status Solidi - Rapid Research Letters, 2021, 15, 2000589.	2.4	23
14	Preparation of 1Âμm thick Y-doped HfO <sub>2</sub> ferroelectric films on (111)Pt/TiO <sub>x</sub> /SiO <sub>2</sub> /(001)Si substrates by a sputtering method and their ferroelectric and piezoelectric properties. Japanese Journal of Applied Physics, 2021, 60, 031009.	1.5	9
15	Large thermal hysteresis of ferroelectric transition in HfO2-based ferroelectric films. Applied Physics Letters, 2021, 118, .	3.3	19
16	Electricâ€Fieldâ€Induced Ferroelectricity in 5%Yâ€doped Hf <sub>0.5</sub> Zr <sub>0.5</sub> O <sub>2</sub> : Transformation from the Paraelectric Tetragonal Phase to the Ferroelectric Orthorhombic Phase. Physica Status Solidi - Rapid Research Letters, 2021, 15, 2170023.	2.4	1
17	Local C-V Characterization for Ferroelectric Films. , 2021, , .		0
18	Comprehensive Study on the Kinetic Formation of the Orthorhombic Ferroelectric Phase in Epitaxial Y-Doped Ferroelectric HfO <sub>2</sub> Thin Films. ACS Applied Electronic Materials, 2021, 3, 3123-3130.	4.3	32

#	Article	IF	CITATIONS
19	Growth of 0.1(Bi,Na)TiO <sub>3</sub> –0.9BaTiO <sub>3</sub> epitaxial films by pulsed laser deposition and their electric properties. Journal of the Ceramic Society of Japan, 2021, 129, 337-342.	1.1	2
20	Impact of Deposition Temperature on Crystal Structure and Ferroelectric Properties of (Al <sub>1â^'<i>x</i></sub> Sc <sub><i>x</i></sub> )N Films Prepared by Sputtering Method. Physica Status Solidi (A) Applications and Materials Science, 2021, 218, 2100302.	1.8	6
21	Influence of cooling rate on ferroelastic domain structure for epitaxial (100)/(001)-oriented Pb(Zr,) Tj ETQq1 1 0.	784314 rg 1.5	gBT /Overlock
22	High-precision local C–V mapping for ferroelectrics using principal component analysis. Japanese Journal of Applied Physics, 2021, 60, SFFB09.	1.5	1
23	Thickness scaling of (Al <sub>0.8</sub> Sc <sub>0.2</sub> )N films with remanent polarization beyond 100ÂμCÂcm <sup>â^²2</sup> around 10Ânm in thickness. Applied Physics Express, 2021, 14, 105501.	2.4	30
24	Domain structure transition in compressively strained (100)/(001) epitaxial tetragonal PZT film. Journal of Applied Physics, 2021, 129, 024101.	2.5	2
25	Multi-Omics Analysis to Generate Hypotheses for Mild Health Problems in Monkeys. Metabolites, 2021, 11, 701.	2.9	0
26	Demonstration of ferroelectricity in ScGaN thin film using sputtering method. Applied Physics Letters, 2021, 119, .	3.3	15
27	Composition dependencies of crystal structure and electrical properties of epitaxial tetragonal (Bi,) Tj ETQq1 1 0 depositions. Journal of Applied Physics, 2021, 130, .	.784314 rg 2.5	gBT /Overlo <mark>c</mark> i 3
28	Development of Tandem Mass Tag Labeling Method for Lipid Molecules Containing Carboxy and Phosphate Groups, and Their Stability in Human Serum. Metabolites, 2021, 11, 19.	2.9	3
29	Mitochondrial complex I inhibitors suppress tumor growth through concomitant acidification of the intra- and extracellular environment. IScience, 2021, 24, 103497.	4.1	17
30	Thickness dependence of phase stability in epitaxial <mml:math xmlns:mml="http://www.w3.org/1998/Math/MathML"&gt;<mml:mrow><mml:mrow><mml:mo>(</mml:mo><mml:n mathvariant="normal"&gt;O<mml:mn>2</mml:mn></mml:n </mml:mrow> films. Physical Review Materials, 2021, 5, .</mml:mrow></mml:math 	nsub> <mn 2.4</mn 	nl:mi>Hf
31	Large Piezoelectric Response in Lead-Free (Bi <sub>0.5</sub> Na <sub>0.5</sub> )TiO <sub>3</sub> -Based Perovskite Thin Films by Ferroelastic Domain Switching: Beyond the Morphotropic Phase Boundary Paradigm. ACS Applied Materials & Interfaces, 2021, 13, 57532-57539.	8.0	8
32	Nax-positive glial cells in the organum vasculosum laminae terminalis produce epoxyeicosatrienoic acids to induce water intake in response to increases in [Na+] in body fluids. Neuroscience Research, 2020, 154, 45-51.	1.9	10
33	Epitaxial growth of Mg <sub>2</sub> Si films on (111) Si substrates covered with epitaxial SiC layers. Japanese Journal of Applied Physics, 2020, 59, SF1001.	1.5	4
34	The Atlas of Inflammation Resolution (AIR). Molecular Aspects of Medicine, 2020, 74, 100894.	6.4	110
35	Good piezoelectricity of self-polarized thick epitaxial (K,Na)NbO3 films grown below the Curie temperature (240 °C) using a hydrothermal method. Applied Physics Letters, 2020, 117, .	3.3	8
36	Effects of deposition conditions on the ferroelectric properties of (Al1â~' <i>x</i> Sc <i>x</i> )N thin films. Journal of Applied Physics, 2020, 128, .	2.5	127

#	Article	IF	CITATIONS
37	Hepatic Levels of DHA-Containing Phospholipids Instruct SREBP1-Mediated Synthesis and Systemic Delivery of Polyunsaturated Fatty Acids. IScience, 2020, 23, 101495.	4.1	26
38	Composition Dependence of Crystal Structures and Electrical Properties of Ca-Mg-Si Films Prepared by Sputtering. Journal of Electronic Materials, 2020, 49, 7509-7517.	2.2	1
39	A computational search for wurtzite-structured ferroelectrics with low coercive voltages. APL Materials, 2020, 8, .	5.1	19
40	Epitaxial Crystal Growth of Bismuth Silicate Driven by Fluorite-like Layers. Crystal Growth and Design, 2020, 20, 7163-7169.	3.0	2
41	Fabrication and characterization of (CaxSr1-x)Si2 films prepared by co-sputtering method. MRS Advances, 2020, 5, 451-458.	0.9	0
42	Large Electromechanical Responses Driven by Electrically Induced Dense Ferroelastic Domains: Beyond Morphotropic Phase Boundaries. ACS Applied Electronic Materials, 2020, 2, 1908-1916.	4.3	11
43	Roles of polyunsaturated fatty acids, from mediators to membranes. Journal of Lipid Research, 2020, 61, 1150-1160.	4.2	83
44	Lysophosphatidylethanolamine acyltransferase 2 (LPEAT2) incorporates DHA into phospholipids and has possible functions for fatty acid-induced cell death. Biochemical and Biophysical Research Communications, 2020, 526, 246-252.	2.1	22
45	Fabrication and characterization of ReO3-type dielectric films. Journal of Materials Chemistry C, 2020, 8, 4680-4684.	5.5	0
46	Temperature dependence on the domain structure of epitaxial PbTiO <sub>3</sub> films grown on single crystal substrates with different lattice parameters. Japanese Journal of Applied Physics, 2020, 59, SPPB01.	1.5	8
47	Thickness- and orientation- dependences of Curie temperature in ferroelectric epitaxial Y doped HfO <sub>2</sub> films. Japanese Journal of Applied Physics, 2020, 59, SGGB04.	1.5	22
48	Thermoelectric (Ba x Sr1–x )Si2 films prepared by sputtering method over the barium solubility limit. Japanese Journal of Applied Physics, 2020, 59, SFFB02.	1.5	4
49	Limitations of deuterium″abeled internal standards for quantitative electrospray ionization mass spectrometry analysis of fatty acid metabolites. Rapid Communications in Mass Spectrometry, 2020, 34, e8814.	1.5	7
50	Room-temperature deposition of ferroelectric HfO2-based films by the sputtering method. Applied Physics Letters, 2020, 116, .	3.3	28
51	Local C–V mapping for ferroelectrics using scanning nonlinear dielectric microscopy. Journal of Applied Physics, 2020, 128, 244105.	2.5	4
52	Preparation of near-1-µm-thick {100}-oriented epitaxial Y-doped HfO <sub>2</sub> ferroelectric films on (100)Si substrates by a radio-frequency magnetron sputtering method. Journal of the Ceramic Society of Japan, 2020, 128, 539-543.	1.1	14
53	High yield preparation of (100) <i><sub>c</sub></i> -oriented (K,Na)NbO <sub>3</sub> thick films by hydrothermal method using amorphous niobium source. Journal of the Ceramic Society of Japan, 2020, 128, 512-517.	1.1	9
54	Rapid deposition of (K,Na)NbO3 thick films using microwave-assisted hydrothermal technique. Japanese Journal of Applied Physics, 2020, 59, SPPB02.	1.5	7

#	Article	IF	CITATIONS
55	Dependency of direct and inverse transverse piezoelectric properties on composition in self-polarized epitaxial (K <sub><i>x</i>kub&gt;Na<sub>1â^'<i>x</i>kub&gt;NbO<sub>3</sub>films grown via a hydrothermal method. Japanese Journal of Applied Physics, 2020, 59, SPPC03.</sub></sub>	1.5	10
56	Crystal structure, ferroelectric and piezoelectric properties of epitaxial (1â^' <i>x</i> )(Bi <sub>0.5</sub> Na <sub>0.5</sub> )TiO <sub>3</sub> – <i>x</i> (Bi <sub>0.5</sub> K <sub>0.5</sub> films grown by hydrothermal method. Japanese Journal of Applied Physics, 2020, 59, SPPB10.	/suþ>)TiO	<suoob>3</suoob>
57	Optimization of deposition conditions of yttrium doped-SrZrO <sub>3</sub> thin films fabricated by pulsed laser deposition. Journal of the Ceramic Society of Japan, 2020, 128, 436-440.	1.1	4
58	Quantification of Fatty Acids in Mammalian Tissues by Gas Chromatography–Hydrogen Flame Ionization Detection. Bio-protocol, 2020, 10, e3613.	0.4	3
59	Cytosolic phospholipase A2 and lysophospholipid acyltransferases. Biochimica Et Biophysica Acta - Molecular and Cell Biology of Lipids, 2019, 1864, 838-845.	2.4	54
60	Ferroelectric properties of epitaxial Bi <sub>2</sub> SiO <sub>5</sub> thin films grown on SrTiO <sub>3</sub> substrates with various orientations. Japanese Journal of Applied Physics, 2019, 58, SLLB04.	1.5	5
61	Ferroelectricity in YO1.5-HfO2 films around 1 <i>μ</i> m in thickness. Applied Physics Letters, 2019, 115, .	3.3	53
62	Evaluation of phase and thermoelectric properties of thin film SrSi <sub>2</sub> . Journal of the Ceramic Society of Japan, 2019, 127, 394-398.	1.1	6
63	Environmental Optimization Enables Maintenance of Quiescent Hematopoietic Stem Cells ExÂVivo. Cell Reports, 2019, 28, 145-158.e9.	6.4	54
64	Polyunsaturated fatty acids promote <i>Plasmodium falciparum</i> gametocytogenesis. Biology Open, 2019, 8, .	1.2	11
65	Electric field-induced change in the crystal structure of MOCVD-Pb(Zr,Ti)O3 films near the phase boundary. Japanese Journal of Applied Physics, 2019, 58, SLLB07.	1.5	2
66	Growth of epitaxial (K, Na)NbO3 films with various orientations by hydrothermal method and their properties. Japanese Journal of Applied Physics, 2019, 58, SLLB14.	1.5	11
67	xmlns:mml="http://www.w3.org/1998/Math/MathML"> < mml:mrow> < mml:mrow> < mml:mo> ( < /mml:mo> < mml:m rhombohedral epitaxial < mml:math xmlns:mml="http://www.w3.org/1998/Math/MathML"> < mml:mrow> < mml:mi> Pb < /mml:mi> < mml:mrow> <.	n>1113.2	nml:mn> <mr 3</mr 
68	Effects of starting materials on the deposition behavior of hydrothermally synthesized {1 0 0} -oriented epitaxial (K,Na)NbO3 thick films and their ferroelectric and piezoelectric properties. Journal of Crystal Growth, 2019, 511, 1-7.	1.5	18
69	Characterization of supported liquid extraction as a sample pretreatment method for eicosanoids and related metabolites in biological fluids. Journal of Chromatography B: Analytical Technologies in the Biomedical and Life Sciences, 2019, 1124, 298-307.	2.3	14
70	Formation of the orthorhombic phase in CeO2-HfO2 solid solution epitaxial thin films and their ferroelectric properties. Applied Physics Letters, 2019, 114, .	3.3	30
71	Preparation of CaMgSi and Ca7Mg7.25Si14 single phase films and their thermoelectric properties. MRS Advances, 2019, 4, 1503-1508.	0.9	3
72	Role of the high-affinity leukotriene B4 receptor signaling in fibrosis after unilateral ureteral obstruction in mice. PLoS ONE, 2019, 14, e0202842.	2.5	11

#	Article	IF	Citations
73	Effects of heat treatment and in situ high-temperature X-ray diffraction study on the formation of ferroelectric epitaxial Y-doped HfO <sub>2</sub> film. Japanese Journal of Applied Physics, 2019, 58, SBBB09.	1.5	34
74	Epitaxial Growth of Doped HfO2 Ferroelectric Materials. , 2019, , 173-192.		3
75	Structural Origin of Temperature-Dependent Ferroelectricity. , 2019, , 193-216. Electric-Field-Driven Nanosecond Ferroelastic-Domain Switching Dynamics in Epitaxial <mml:math< td=""><td></td><td>2</td></mml:math<>		2
76	xmlns:mml="http://www.w3.org/1998/Math/MathML" display="inline"> <mml:mrow><mml:mi>Pb</mml:mi><mml:mo stretchy="false"&gt;(<mml:mi>Zr</mml:mi><mml:mo>,</mml:mo><mml:mi>Ti</mml:mi><ml:mo) e<="" td="" tj=""><td>.TQq0 0 0</td><td>rg<mark>16</mark> /Overloc</td></ml:mo)></mml:mo </mml:mrow>	.TQq0 0 0	rg <mark>16</mark> /Overloc
77	mathvariant="normal">O <mml:mrow><mml:mn>3</mml:mn></mml:mrow> Deposition of orientation-controlled thick (K,Na)NbO&tsub>3⁢/sub> films on metal substrates by repeated hydrothermal deposition technique. Journal of the Ceramic Society of Japan, 2019, 127, 478-484.	b> < /mml: 1.1	mrow>7
78	Isobaric mass tagging and triple quadrupole mass spectrometry to determine lipid biomarker candidates for Alzheimer's disease. PLoS ONE, 2019, 14, e0226073.	2.5	21
79	Control of p- and n-type Conduction in Thermoelectric Non-doped Mg2Si Thin Films Prepared by Sputtering Method. MRS Advances, 2018, 3, 1355-1359.	0.9	5
80	Growth of (111)-oriented epitaxial magnesium silicide (Mg2Si) films on (001) Al2O3 substrates by RF magnetron sputtering and their properties. Journal of Materials Science, 2018, 53, 5151-5158.	3.7	8
81	Na+-mimicking ligands stabilize the inactive state of leukotriene B4 receptor BLT1. Nature Chemical Biology, 2018, 14, 262-269.	8.0	80
82	Ferroelectricity mediated by ferroelastic domain switching in HfO2-based epitaxial thin films. Applied Physics Letters, 2018, 113, .	3.3	69
83	Formation of polar phase in Fe-doped ZrO2 epitaxial thin films. Applied Physics Letters, 2018, 113, .	3.3	8
84	Domain structure transition from two to three dimensions in tensile strained (100)/(001)-oriented epitaxial tetragonal PZT film. Applied Physics Letters, 2018, 113, .	3.3	8
85	Epitaxial ferroelectric Y-doped HfO <sub>2</sub> film grown by the RF magnetron sputtering. Japanese Journal of Applied Physics, 2018, 57, 11UF15.	1.5	15
86	Domain orientation relationship of orthorhombic and coexisting monoclinic phases of YO <sub>1.5</sub> -doped HfO <sub>2</sub> epitaxial thin films. Japanese Journal of Applied Physics, 2018, 57, 11UF16.	1.5	16
87	Thickness-dependent crystal structure and electric properties of epitaxial ferroelectric Y2O3-HfO2 films. Applied Physics Letters, 2018, 113, .	3.3	48
88	Fabrication of ferroelectric Fe doped HfO <sub>2</sub> epitaxial thin films by ion-beam sputtering method and their characterization. Japanese Journal of Applied Physics, 2018, 57, 11UF02.	1.5	23
89	Epitaxial growth of perovskite-type oxide thin film on (111)SrTiO <sub>3</sub> substrate using (101)PdO as a buffer layer. Japanese Journal of Applied Physics, 2018, 57, 11UF04.	1.5	2
90	Ferroelectricity in HfO <sub>2</sub> and related ferroelectrics. Journal of the Ceramic Society of Japan, 2018, 126, 667-674.	1.1	22

Τακάο Shimizu

#	Article	IF	CITATIONS
91	Lysophosphatidic acid receptor, LPA6, regulates endothelial blood-brain barrier function: Implication for hepatic encephalopathy. Biochemical and Biophysical Research Communications, 2018, 501, 1048-1054.	2.1	27
92	Stability of the orthorhombic phase in (111)-oriented YO <sub>1.5</sub> -substituted HfO <sub>2</sub> films. Journal of the Ceramic Society of Japan, 2018, 126, 269-275.	1.1	8
93	Time response demonstration of in situ lattice deformation under an applied electric field by synchrotron-based time-resolved X-ray diffraction in polar-axis-oriented epitaxial Pb(Zr,Ti)O3 film. Japanese Journal of Applied Physics, 2018, 57, 0902B8.	1.5	2
94	Stepwise phosphorylation of leukotriene B <sub>4</sub> receptor 1 defines cellular responses to leukotriene B <sub>4</sub> . Science Signaling, 2018, 11, .	3.6	15
95	The Gα12/13-coupled receptor LPA4 limits proper adipose tissue expansion and remodeling in diet-induced obesity. JCI Insight, 2018, 3, .	5.0	22
96	Leukotriene receptors as potential therapeutic targets. Journal of Clinical Investigation, 2018, 128, 2691-2701.	8.2	129
97	Phospholipid metabolism in health and disease. Proceedings for Annual Meeting of the Japanese Pharmacological Society, 2018, WCP2018, CL-31.	0.0	0
98	Preparation of preferentially (111)-oriented Mg <sub>2</sub> Si thin films on (001)Al <sub>2</sub> O <sub>3</sub> and (100)CaF <sub>2</sub> substrates and their thermoelectric properties. Japanese Journal of Applied Physics, 2017, 56, 05DC02.	1.5	9
99	Docosahexaenoic acid preserves visual function by maintaining correct disc morphology in retinal photoreceptor cells. Journal of Biological Chemistry, 2017, 292, 12054-12064.	3.4	113
100	Lysophosphatidic acid acyltransferase 3 tunes the membrane status of germ cells by incorporating docosahexaenoic acid during spermatogenesis. Journal of Biological Chemistry, 2017, 292, 12065-12076.	3.4	53
101	Crystal structure and dielectric/ferroelectric properties of CSD-derived HfO 2 -ZrO 2 solid solution films. Ceramics International, 2017, 43, S501-S505.	4.8	24
102	Effect of in-plane tensile strain in (100)/(001)-oriented epitaxial PbTiO3 films on their phase transition temperature and tetragonal distortion. Applied Physics Letters, 2017, 110, .	3.3	10
103	Mediator lipidomics by liquid chromatography-tandem mass spectrometry. Biochimica Et Biophysica Acta - Molecular and Cell Biology of Lipids, 2017, 1862, 777-781.	2.4	6
104	Effect of the film thickness on the crystal structure and ferroelectric properties of (Hf 0.5 Zr 0.5 )O 2 thin films deposited on various substrates. Materials Science in Semiconductor Processing, 2017, 70, 239-245.	4.0	41
105	Orchestrating Role of Apoptosis Inhibitor of Macrophage in the Resolution of Acute Lung Injury. Journal of Immunology, 2017, 199, 3870-3882.	0.8	23
106	Multiplex quantitative analysis of eicosanoid mediators in human plasma and serum: Possible introduction into clinical testing. Journal of Chromatography B: Analytical Technologies in the Biomedical and Life Sciences, 2017, 1068-1069, 98-104.	2.3	17
107	Dynamic observation of ferroelectric domain switching using scanning nonlinear dielectric microscopy. Japanese Journal of Applied Physics, 2017, 56, 10PF16.	1.5	4
108	Electric-field-induced lattice distortion in epitaxial BiFeO3 thin films as determined by <i>in situ</i> time-resolved x-ray diffraction. Applied Physics Letters, 2017, 111, .	3.3	3

#	Article	IF	CITATIONS
109	In-situ observation of ultrafast 90° domain switching under application of an electric field in (100)/(001)-oriented tetragonal epitaxial Pb(Zr0.4Ti0.6)O3 thin films. Scientific Reports, 2017, 7, 9641.	3.3	23
110	Crystal structure and magnetism in κ-Al2O3-type AlxFe2-xO3 films on SrTiO3(111). Journal of Applied Physics, 2017, 122, 015301.	2.5	14
111	Epitaxial growth of YO <sub>1.5</sub> doped HfO <sub>2</sub> films on (100) YSZ substrates with various concentrations. Ferroelectrics, 2017, 512, 105-110.	0.6	10
112	Lysophosphatidylcholine acyltransferase 4 is involved in chondrogenic differentiation of ATDC5 cells. Scientific Reports, 2017, 7, 16701.	3.3	18
113	Orientation change with substrate type and composition in (100)/(001)-oriented epitaxial tetragonal Pb(Zr <i><sub>x</sub></i> Ti <sub>1−</sub> <i><sub>x</sub></i> )O <sub>3</sub> films. Journal of the Ceramic Society of Japan, 2017, 125, 458-462.	1.1	3
114	Lysophosphatidylethanolamine acyltransferase 1/membraneâ€bound <i>O</i> â€acyltransferase 1 regulates morphology and function of P19C6 cellâ€derived neurons. FASEB Journal, 2016, 30, 2591-2601.	0.5	8
115	Thermally stable dielectric responses in uniaxially (001)-oriented CaBi4Ti4O15 nanofilms grown on a Ca2Nb3O10â^ nanosheet seed layer. Scientific Reports, 2016, 6, 20713.	3.3	8
116	Mechanism of polarization switching in wurtzite-structured zinc oxide thin films. Applied Physics Letters, 2016, 109, .	3.3	30
117	Impact of mechanical stress on ferroelectricity in (Hf0.5Zr0.5)O2 thin films. Applied Physics Letters, 2016, 108, .	3.3	187
118	Simultaneous achievement of high dielectric constant and low temperature dependence of capacitance in (111)-oriented BaTiO3-Bi(Mg0.5Ti0.5)O3-BiFeO3 solid solution thin films. AIP Advances, 2016, 6, .	1.3	4
119	Evidence of ferroelectricity in ferrimagnetic <i>κ</i> -Al2O3-type In0.25Fe1.75O3 films. Applied Physics Letters, 2016, 109, .	3.3	15
120	Crystal structure and compositional analysis of epitaxial (K <sub>0.56</sub> Na <sub>0.44</sub> )NbO <sub>3</sub> films prepared by hydrothermal method. Journal of Materials Research, 2016, 31, 693-701.	2.6	7
121	Growth of (111)-oriented epitaxial and textured ferroelectric Y-doped HfO2 films for downscaled devices. Applied Physics Letters, 2016, 109, .	3.3	62
122	Orientation control and domain structure analysis of {100}-oriented epitaxial ferroelectric orthorhombic HfO2-based thin films. Journal of Applied Physics, 2016, 119, .	2.5	57
123	Formation of (111) orientation-controlled ferroelectric orthorhombic HfO2 thin films from solid phase via annealing. Applied Physics Letters, 2016, 109, .	3.3	29
124	Fabrication and characterization of (111)-epitaxial Pb(Zr0.35Ti0.65)O3/Pb(Zr0.65Ti0.35)O3artificial superlattice thin films. Japanese Journal of Applied Physics, 2016, 55, 10TA20.	1.5	2
125	High temperature stability of the dielectric and insulating properties of Ca(Ti, Zr)SiO5 ceramics. Applied Physics Letters, 2016, 108, .	3.3	11
126	Transport Properties of CuNb/Nb <sub>3</sub> Sn Rutherford Coils With Various Diameters. IEEE Transactions on Applied Superconductivity, 2016, 26, 1-4.	1.7	3

#	Article	IF	CITATIONS
127	Imaging of intracellular fatty acids by scanning Xâ€ray fluorescence microscopy. FASEB Journal, 2016, 30, 4149-4158.	0.5	22
128	Crystal Isomers of ScFeO <sub>3</sub> . Crystal Growth and Design, 2016, 16, 5214-5222.	3.0	25
129	Growth of epitaxial tetragonal (Bi,K)TiO3films and their ferroelectric and piezoelectric properties. Japanese Journal of Applied Physics, 2016, 55, 10TA13.	1.5	8
130	The demonstration of significant ferroelectricity in epitaxial Y-doped HfO2 film. Scientific Reports, 2016, 6, 32931.	3.3	194
131	Preparation of Ca-Si Films on (001) Al2O3 Substrates by an RF Magnetron Sputtering Method and Their Electrical Properties. Journal of Electronic Materials, 2016, 45, 3121-3126.	2.2	6
132	Growth of {110}-one-axis-oriented perovskite-type oxide films using self-aligned epitaxial (101)PdO//(111) Pd double layers. Thin Solid Films, 2016, 599, 133-137.	1.8	6
133	Lysophosphatidylcholine acyltransferase 1 protects against cytotoxicity induced by polyunsaturated fatty acids. FASEB Journal, 2016, 30, 2027-2039.	0.5	24
134	The leukotriene B4 receptor BLT1 is stabilized by transmembrane helix capping mutations. Biochemistry and Biophysics Reports, 2015, 4, 243-249.	1.3	2
135	Domain structure of tetragonal Pb(Zr,Ti)O <sub>3</sub> nanorods and its size dependence. Japanese Journal of Applied Physics, 2015, 54, 10NA07.	1.5	8
136	Negligible substrate clamping effect on piezoelectric response in (111)-epitaxial tetragonal Pb(Zr, Ti)O3 films. Journal of Applied Physics, 2015, 118, .	2.5	21
137	Predominant Role of Cytosolic Phospholipase A2α in Dioxin-induced Neonatal Hydronephrosis in Mice. Scientific Reports, 2015, 4, 4042.	3.3	10
138	Orientation control of epitaxial tetragonal Pb(ZrxTi1â^'x)O3 thin films grown on (100)KTaO3 substrates by tuning the Zr/(Zr + Ti) ratio. Applied Physics Letters, 2015, 107, .	3.3	11
139	Fabrication of tetragonal Pb(Zr,Ti)O <inf>3</inf> nanorods by focused ion beam and characterization of the domain structure. , 2015, , .		2
140	Raman Tensor Analysis by Angle-Resolved Polarized Spectroscopy. Nihon Kessho Gakkaishi, 2015, 57, 285-290.	0.0	0
141	Essential Role of Lysophosphatidylcholine Acyltransferase 3 in the Induction of Macrophage Polarization in PMAâ€Treated U937 Cells. Journal of Cellular Biochemistry, 2015, 116, 2840-2848.	2.6	42
142	Fever Is Mediated by Conversion of Endocannabinoid 2-Arachidonoylglycerol to Prostaglandin E2. PLoS ONE, 2015, 10, e0133663.	2.5	30
143	Role of p38 mitogenâ€activated protein kinase in linking stearoylâ€CoA desaturaseâ€1 activity with endoplasmic reticulum homeostasis. FASEB Journal, 2015, 29, 2439-2449.	0.5	35
144	Contribution of oxygen vacancies to the ferroelectric behavior of Hf0.5Zr0.5O2 thin films. Applied Physics Letters, 2015, 106, .	3.3	65

#	Article	IF	CITATIONS
145	A comprehensive quantification method for eicosanoids and related compounds by using liquid chromatography/mass spectrometry with high speed continuous ionization polarity switching. Journal of Chromatography B: Analytical Technologies in the Biomedical and Life Sciences, 2015, 995-996, 74-84.	2.3	63
146	Transport Properties of CuNb Reinforced <inline-formula> <tex-math notation="TeX"&gt;\$hbox{Nb}_{3}hbox{Sn}\$</tex-math </inline-formula> Rutherford Coils in High Fields. IEEE Transactions on Applied Superconductivity, 2015, 25, 1-4.	1.7	9
147	Local structure and molecular motions in imidazolium hydrogen malonate crystal as studied by 2H and 13C NMR. Hyperfine Interactions, 2015, 230, 95-100.	0.5	4
148	The atypical Nâ€glycosylation motif, Asn ys ys, in human GPR109A is required for normal cell surface expression and intracellular signaling. FASEB Journal, 2015, 29, 2412-2422.	0.5	13
149	Establishment of LC-MS methods for the analysis of palmitoylated surfactant proteins. Journal of Lipid Research, 2015, 56, 1370-1379.	4.2	4
150	The Absence of the Leukotriene B <sub>4</sub> Receptor BLT1 Attenuates Peripheral Inflammation and Spinal Nociceptive Processing Following Intraplantar Formalin Injury. Molecular Pain, 2015, 11, s12990-015-0010.	2.1	18
151	Stabilizing the ferroelectric phase in doped hafnium oxide. Journal of Applied Physics, 2015, 118, .	2.5	424
152	Growth of epitaxial orthorhombic YO1.5-substituted HfO2 thin film. Applied Physics Letters, 2015, 107, .	3.3	123
153	Fatty acid remodeling by LPCAT3 enriches arachidonate in phospholipid membranes and regulates triglyceride transport. ELife, 2015, 4, .	6.0	161
154	Rapid Production of Platelet-activating Factor Is Induced by Protein Kinase Cα-mediated Phosphorylation of Lysophosphatidylcholine Acyltransferase 2 Protein. Journal of Biological Chemistry, 2014, 289, 15566-15576.	3.4	31
155	Selective inhibitors of a PAF biosynthetic enzyme lysophosphatidylcholine acyltransferase 2. Journal of Lipid Research, 2014, 55, 1386-1396.	4.2	20
156	Ferroelectricity in wurtzite structure simple chalcogenide. Applied Physics Letters, 2014, 104, .	3.3	52
157	Study on the effect of heat treatment conditions on metalorganic-chemical-vapor-deposited ferroelectric Hf <sub>0.5</sub> Zr <sub>0.5</sub> O <sub>2</sub> thin film on Ir electrode. Japanese Journal of Applied Physics, 2014, 53, 09PA04.	1.5	59
158	<b>Low Temperature Preparation of KNbO</b> <sub>3</sub> <b>Films by Hydrothermal Method and Their Characterization</b> . Materials Research Society Symposia Proceedings, 2014, 1659, 49-54.	0.1	3
159	High Temperature Reproducible Preparation of Mg2Si Films on (001)Al2O3 substrates Using RF Magnetron Sputtering Method. Materials Research Society Symposia Proceedings, 2014, 1642, 1.	0.1	6
160	Electrical Properties of (110)-Oriented Nondoped Mg2Si Films with p-Type Conduction Prepared by RF Magnetron Sputtering Method. Journal of Electronic Materials, 2014, 43, 2269-2273.	2.2	25
161	A novel lysophosphatidic acid acyltransferase enzyme (LPAAT4) with a possible role for incorporating docosahexaenoic acid into brain glycerophospholipids. Biochemical and Biophysical Research Communications, 2014, 443, 718-724.	2.1	57
162	Lead- and alkali-metal-free BaTiO3–Bi(Mg0.5Ti0.5)O3–BiFeO3solid-solution thin films with high dielectric constant prepared on Si substrates by solution-based method. Japanese Journal of Applied Physics, 2014, 53, 09PA12.	1.5	4

#	Article	IF	CITATIONS
163	Lysophospholipid Acyltransferases Mediate Phosphatidylcholine Diversification to Achieve the Physical Properties Required InÂVivo. Cell Metabolism, 2014, 20, 295-305.	16.2	133
164	Epitaxial growth of metastable multiferroic AlFeO <sub>3</sub> film on SrTiO <sub>3</sub> (111) substrate. Applied Physics Letters, 2014, 104, 082906.	3.3	44
165	Raman Tensor Analysis of Crystalline Lead Titanate by Quantitative Polarized Spectroscopy. Ferroelectrics, 2014, 462, 8-13.	0.6	22
166	Structural Modification and Domain Structure in a BaTiO <sub>3</sub> Film on (110) SrTiO <sub>3</sub> . Applied Physics Express, 2013, 6, 015803.	2.4	11
167	Differential cellular localization of antioxidant enzymes in the trigeminal ganglion. Neuroscience, 2013, 248, 345-358.	2.3	51
168	Comparative study of phase transitions in BaTiO <sub>3</sub> thin films grown on (001)- and (110)-oriented SrTiO <sub>3</sub> substrate. Journal of Physics Condensed Matter, 2013, 25, 132001.	1.8	23
169	Crystal Structure Analysis of Hydrothermally Synthesized Epitaxial (K <sub>x</sub> Na <sub>1-x</sub> )NbO <sub>3</sub> Films. Japanese Journal of Applied Physics, 2013, 52, 09KA11.	1.5	22
170	Unconventional Structure in BaTiO3 Thin Film Grown on ï¼^110)SrTiO3 Substrate. Nihon Kessho Gakkaishi, 2013, 55, 290-295.	0.0	0
171	Feasibility, Safety, and Therapeutic Efficacy of Human Induced Pluripotent Stem Cell-Derived Cardiomyocyte Sheets in a Porcine Ischemic Cardiomyopathy Model. Circulation, 2012, 126, S29-37.	1.6	421
172	Origin of the dielectric response in Ba0.767Ca0.233TiO3. Applied Physics Letters, 2012, 100, .	3.3	14
173	Leukotriene Receptors. Chemical Reviews, 2011, 111, 6231-6298.	47.7	75
174	Mechanism for suppression of ferroelectricity in Cd1â^'xCaxTiO3. Physical Review B, 2011, 84, .	3.2	40
175	Development of a Flux Stabilizer for NMR Measurements with a Hybrid Magnet. Journal of Low Temperature Physics, 2010, 159, 288-291.	1.4	1
176	Lipid signaling in cytosolic phospholipase A <sub>2</sub> α–cyclooxygenase-2 cascade mediates cerebellar long-term depression and motor learning. Proceedings of the National Academy of Sciences of the United States of America, 2010, 107, 3198-3203.	7.1	48
177	The Endocannabinoid 2-Arachidonoylglycerol Produced by Diacylglycerol Lipase α Mediates Retrograde Suppression of Synaptic Transmission. Neuron, 2010, 65, 320-327.	8.1	407
178	Phonon Dynamics in BiFeO <sub>3</sub> Studied by Raman Scattering. Ferroelectrics, 2010, 403, 187-190.	0.6	8
179	Role of lysophosphatidic acid acyltransferase 3 for the supply of highly polyunsaturated fatty acids in TM4 Sertoli cells. FASEB Journal, 2010, 24, 4929-4938.	0.5	15
180	Helix 8 for ER Export of Leukotriene B 4 typeâ€⊋ Receptor (BLT2). FASEB Journal, 2010, 24, lb87.	0.5	0

ΤΑΚΑΟ SHIMIZU

#	Article	IF	CITATIONS
181	The expression of leukotriene B 4 typeâ€l receptor, BLT1, is facilitated by AML1 in leukocytes. FASEB Journal, 2010, 24, lb58.	0.5	0
182	Protective role of the leukotriene B4receptor BLT2 in murine inflammatory colitis. FASEB Journal, 2010, 24, 4678-4690.	0.5	14
183	Lipid Mediators in Health and Disease: Enzymes and Receptors as Therapeutic Targets for the Regulation of Immunity and Inflammation. Annual Review of Pharmacology and Toxicology, 2009, 49, 123-150.	9.4	499
184	Ferroelectric phase transition of <mml:math <br="" xmlns:mml="http://www.w3.org/1998/Math/MathML">display="inline"&gt;<mml:mrow><mml:msub><mml:mrow><mml:mtext>Cd</mml:mtext></mml:mrow><mml:mn>2 by Raman scattering. Physical Review B, 2008, 77, .</mml:mn></mml:msub></mml:mrow></mml:math>	2< <b>βn₂</b> ml:m	n> <b>≭¢</b> mml:ms⊧
185	Reduced pain behaviors and extracellular signalâ€related protein kinase activation in primary sensory neurons by peripheral tissue injury in mice lacking plateletâ€activating factor receptor. Journal of Neurochemistry, 2007, 102, 1658-1668.	3.9	29
186	Cytosolic Phospholipase A2α (cPLA2α) Functions at the Nexus of Bidirectional Integrin Signaling in Platelets Blood, 2007, 110, 136-136.	1.4	2
187	Sensory system-predominant distribution of leukotriene A4 hydrolase and its colocalization with calretinin in the mouse nervous system. Neuroscience, 2006, 141, 917-927.	2.3	14
188	Cytosolic phospholipase A 2 : Biochemical properties and physiological roles. IUBMB Life, 2006, 58, 328-333.	3.4	84
189	A comprehensive classification system for lipids. European Journal of Lipid Science and Technology, 2005, 107, 337-364.	1.5	94
190	Nuclear Spin Polarizer for Solid-State NMR Quantum Computers. AIP Conference Proceedings, 2005, , .	0.4	0
191	Effect of bone marrow transplantation of cytosolic phospholipase A2 deficient mice in focal cerebral ischemia/reperfusion injury. Journal of Cerebral Blood Flow and Metabolism, 2005, 25, S501-S501.	4.3	1
192	Effective Extraction and Analysis for Lysophosphatidic Acids and Their Precursors in Human Plasma Using Electrospray Ionization Mass Spectrometry. Journal of the Mass Spectrometry Society of Japan, 2005, 53, 217-226.	0.1	8
193	Specific Detection of Lysophosphatidic Acids in Serum Extracts by Tandem Mass Spectrometry. Journal of the Mass Spectrometry Society of Japan, 2005, 53, 25-32.	0.1	5
194	PLATELET ACTIVATING FACTOR AFFECTS INTRACELLULAR CALCIUM CONCENTRATION BY MODULATING L-TYPE CALCIUM CHANNEL. , 2005, , .		0
195	G2A Is a Proton-sensing G-protein-coupled Receptor Antagonized by Lysophosphatidylcholine. Journal of Biological Chemistry, 2004, 279, 42484-42491.	3.4	205
196	Hypocretin levels in patients with primary hypersomnia and OSAS, and secondary hypersomnia due to hypocretin deficiency. Sleep and Biological Rhythms, 2004, 2, S50-S50.	1.0	0
197	Effects of n-3 polyunsaturated fatty acids on indomethacin-induced changes in eicosanoid production and blood flow in the gastric mucosa of rats. Prostaglandins Leukotrienes and Essential Fatty Acids, 2003, 69, 33-37.	2.2	6
198	Nuclear-localization-signal-dependent and nuclear-export-signal-dependent mechanisms determine the localization of 5-lipoxygenase. Biochemical Journal, 2002, 361, 505-514.	3.7	38

#	Article	IF	CITATIONS
199	Investigation of nuclear-spin couplings in the lithium fluorides as possible candidates for crystal nuclear magnetic resonance quantum computing devices. Applied Physics A: Materials Science and Processing, 2002, 74, 73-77.	2.3	6
200	Chemokines in synovial inflammation in rheumatoid arthritis: basic and clinical aspects. Modern Rheumatology, 2002, 12, 93-99.	1.8	4
201	Magnetic Resonance Cholangiopancreatography in Assessing the Cause of Acute Pancreatitis in Children. Pancreas, 2001, 22, 196-199.	1.1	32
202	Immunohistochemical localization of guinea-pig leukotriene B412-hydroxydehydrogenase/15-ketoprostaglandin 13-reductase. FEBS Journal, 2001, 268, 6105-6113.	0.2	16
203	Recombinant Human Interleukin-11 Decreases Severity of Acute Necrotizing Pancreatitis in Mice. Pancreas, 2000, 21, 134-140.	1.1	35
204	Interaction between neurone and microglia mediated by platelet-activating factor. Genes To Cells, 2000, 5, 397-406.	1.2	62
205	Acute lung injury by sepsis and acid aspiration: a key role for cytosolic phospholipase A2. Nature Immunology, 2000, 1, 42-46.	14.5	294
206	Predication of axillary lymph node metastasis by intravenous digital subtraction angiography in breast cancer, its correlation with microvascular density. Breast Cancer Research and Treatment, 2000, 61, 261-269.	2.5	8
207	Expression of lysophosphatidic acid receptor in rat astrocytes: mitogenic effect and expression of neurotrophic genes. Neurochemical Research, 2000, 25, 573-582.	3.3	52
208	Dependence of the Curie temperature on the Diameter of Fe <sub>3</sub> 0 <sub>4</sub> Ultra-fine Particles. Journal of the Magnetics Society of Japan, 2000, 24, 511-514.	0.4	34
209	Calbindin-D28k in cerebrovascular extrinsic innervation system of the rat. Autonomic Neuroscience: Basic and Clinical, 2000, 84, 130-139.	2.8	1
210	Leukotriene-B4 Receptor and Signal Transduction. , 2000, , 125-141.		3
211	Role of cytosolic phospholipase A2 in the production of lipid mediators and histamine release in mouse bone-marrow-derived mast cells. Biochemical Journal, 2000, 352, 311-317.	3.7	39
212	Progressive Dilatation of the Main Pancreatic Duct Using Magnetic Resonance Cholangiopancreatography in a Boy with Chronic Pancreatitis. Journal of Pediatric Gastroenterology and Nutrition, 2000, 30, 102-104.	1.8	6
213	Platelet-derived growth factor induces cellular growth in cultured chick ventricular myocytes. Cardiovascular Research, 1999, 41, 641-653.	3.8	17
214	Platelet-activating factor receptor is not required for long-term potentiation in the hippocampal CA1 region. European Journal of Neuroscience, 1999, 11, 1313-1316.	2.6	37
215	Occurrence and distribution of substance P receptors in the cerebral blood vessels of the rat. Brain Research, 1999, 830, 372-378.	2.2	18
216	Analysis of the genes responsible for the O-antigen synthesis in enterohaemorrhagicEscherichia coliO157. Microbial Pathogenesis, 1999, 26, 235-247.	2.9	18

ΤΑΚΑΟ SHIMIZU

#	Article	IF	CITATIONS
217	Aminopeptidase B is structurally related to leukotriene-A4 hydrolase but is not a bifunctional enzyme with epoxide hydrolase activity. Biochemical Journal, 1999, 339, 497-502.	3.7	30
218	Transfected rat cMOAT is functionally expressed on the apical membrane in Madin-Darby canine kidney (MDCK) cells. Pharmaceutical Research, 1998, 15, 1851-1856.	3.5	22
219	Sequential expression of bone morphogenetic protein, tumor necrosis factor, and their receptors in bone-forming reaction after mouse femoral marrow ablation. Bone, 1998, 23, 127-133.	2.9	41
220	The Future Potential of Eicosanoids and Their Inhibitors in Paediatric Practice. Drugs, 1998, 56, 169-176.	10.9	11
221	Molecular cloning and expression of inducible nitric oxide synthase in chick embryonic ventricular myocytes. Cardiovascular Research, 1998, 38, 405-413.	3.8	16
222	Effect of influenza A virus infection on acid-induced cough response in children with asthma. European Respiratory Journal, 1997, 10, 71-74.	6.7	12
223	Role of cytosolic phospholipase A2 in allergic response and parturition. Nature, 1997, 390, 618-622.	27.8	691
224	A G-protein-coupled receptor for leukotriene B4 that mediates chemotaxis. Nature, 1997, 387, 620-624.	27.8	918
225	Role of MRP family proteins in the export of organic anion compounds from liver and intestine. Drug Metabolism and Pharmacokinetics, 1997, 12, 80-81.	0.0	0
226	Pirfenidone prevents collagen accumulation in the remnant kidney in rats with partial nephrectomy. Kidney International, Supplement, 1997, 63, S239-43.	0.1	26
227	Identification of macrophage migration inhibitory factor (MIF) in human skin and its immunohistochemical localization. FEBS Letters, 1996, 381, 199-202.	2.8	127
228	Sweet Syndrome in a Child with Aplastic Anemia Receiving Recombinant Granulocyte Colony-Stimulating Factor. Journal of Pediatric Hematology/Oncology, 1996, 18, 282-284.	0.6	40
229	Role of ABC transporters for the biliary excretion of organic anions. Drug Metabolism and Pharmacokinetics, 1996, 11, 5098-5099.	0.0	0
230	Platelet-activating factor receptor. Gene structure and tissue-specific regulation. Advances in Experimental Medicine and Biology, 1996, 416, 79-84.	1.6	3
231	<1>Changes in the Level of 7α-Hydroxy-3-oxo-4cholestenoic Acid in Cerebrospinal Fluid after Subarachnoid Hemorrhage. Neurologia Medico-Chirurgica, 1995, 35, 294-297.	2.2	9
232	Indomethacin inhibition of ossification induced by direct current stimulation. Journal of Orthopaedic Research, 1995, 13, 123-131.	2.3	13
233	The mode of ATP-dependent microtubule-kinesin sliding in the auxotonic condition Journal of Experimental Biology, 1995, 198, 1809-1815.	1.7	2
234	Effects of indomethacin on jejunal mucosal blood flow in the infant rat. European Journal of Pediatrics, 1995, 154, 592-593.	2.7	0

#	Article	IF	CITATIONS
235	Roxithromycin Reduces the Degree of Bronchial Hyperresponsiveness in Children With Asthma. Chest, 1994, 106, 458-461.	0.8	72
236	Cloning, expression and tissue distribution of rat platelet-activating-factor-receptor cDNA. FEBS Journal, 1994, 221, 211-218.	0.2	84
237	Distribution and pathway of the cerebrovascular nerve fibers from the otic ganglion in the rat: anterograde tracing study. Journal of the Autonomic Nervous System, 1994, 49, 47-54.	1.9	22
238	Activation of Mitogen-Activated Protein Kinase and Arachidonate Release via Two G Protein-Coupled Receptors Expressed in the Rat Hippocampus. Annals of the New York Academy of Sciences, 1994, 744, 107-125.	3.8	9
239	Activation of Phospholipase D in Chinese Hamster Ovary Cells Expressing Platelet-Activating Factor Receptor1. Journal of Biochemistry, 1994, 116, 882-891.	1.7	35
240	Characterization of prostaglandin F2? receptor of mouse 3T3 fibroblasts and its functional expression inXenopus laevis oocytes. Journal of Cellular Physiology, 1993, 155, 257-264.	4.1	33
241	Two different promoters direct expression of two distinct forms of mRNAs of human platelet-activating factor receptor. FEBS Letters, 1993, 322, 129-134.	2.8	96
242	Platelet-activating factor receptor and signal transduction. Biochemical Pharmacology, 1992, 44, 1001-1008.	4.4	89
243	Leukotriene A4hydrolase, a bifunctional enzyme Distinction of leukotriene A4hydrolase and aminopeptidase activities by site-directed mutagenesis at Glu-297. FEBS Letters, 1992, 309, 353-357.	2.8	46
244	Endotoxin transduces Ca2+signaling via platelet-activating factor receptor. FEBS Letters, 1992, 314, 125-129.	2.8	55
245	Analysis for Cerebrospinal Fluid Proteins by Sodium Dodecyl Sulfate-Polyacrylamide Gel Electrophoresis. Clinical Chemistry, 1992, 38, 2008-2012.	3.2	6
246	HIGHLY SENSITIVE SIMULTANEOUS DETERMINATION OF PROSTAGLANDINS BY USING HPLC/LASER INDUCED FLUORESCENCE (LIF). Analytical Sciences, 1991, 7, 957-958.	1.6	1
247	Biosynthesis and function of leukotriene B4. Immunochemical study of leukotriene A4 hydrolase and identification of putative leukotriene B4 receptor. Advances in Prostaglandin, Thromboxane, and Leukotriene Research, 1991, 21A, 387-94.	0.2	0
248	Arachidonic Acid Cascade and Signal Transduction. Journal of Neurochemistry, 1990, 55, 1-15.	3.9	589
249	Inhibition of both etoposide-induced DNA fragmentation and activation of poly(ADP-ribose) synthesis by zinc ion. Biochemical and Biophysical Research Communications, 1990, 169, 1172-1177.	2.1	75
250	Biosynthesis and functions of leukotriene C4. Advances in Prostaglandin, Thromboxane, and Leukotriene Research, 1990, 20, 46-53.	0.2	3
251	Leukotriene A4 Hydrolase from Guinea Pig Lung: The Presence of Two Catalytically Active Forms1. Journal of Biochemistry, 1989, 105, 261-264.	1.7	25
252	?-Adrenergic activation of the muscarinic K+ channel is mediated by arachidonic acid metabolites. Pflugers Archiv European Journal of Physiology, 1989, 414, 102-104.	2.8	54

#	Article	IF	CITATIONS
253	Arachidonic acid metabolites as intracellular modulators of the G protein-gated cardiac K+ channel. Nature, 1989, 337, 555-557.	27.8	304
254	Effects of Cyclosporin A on Progressive and Regressive Tumors Induced by Two Cancer Lines Derived from a Single Colon Carcinoma Chemically Induced in the Rat. Immunobiology, 1989, 178, 401-415.	1.9	27
255	Synthesis and structural identification of four dihydroxy acids and 11, 12-leukotriene C4 derived from 11, 12-leukotriene A4. FEBS Journal, 1988, 176, 725-731.	0.2	20
256	Participation of Lipoxygenase Products from Arachidonic Acid in the Pathogenesis of Cerebral Vasospasm. Journal of Neurochemistry, 1988, 50, 1145-1150.	3.9	65
257	Expression of human leukotriene A4hydrolase cDNA inEscherichia coli. FEBS Letters, 1988, 229, 279-282.	2.8	30
258	Synthesis of 11,12-leukotriene A4, 11S,12S-oxido-5Z,7E,9E,14Z-eicosatetraenoic acid, a novel leukotriene of the 12-lipoxy genase pathway. FEBS Letters, 1987, 213, 169-173.	2.8	8
259	Effects of a single injection of anti-asialo GM1 serum on natural cytotoxicity and the growth of a regressive colonic tumor in syngeneic rats. International Journal of Cancer, 1987, 40, 676-680.	5.1	21
260	Enzymic Synthesis of Leukotriene B4in Guinea Pig Brain. Journal of Neurochemistry, 1987, 48, 1541-1546.	3.9	47
261	Purification of a new acidic glutathione S-transferase, CST-Yn1 Yn1, with a high leukotriene-C4 synthase activity from rat brain. FEBS Journal, 1987, 170, 159-164.	0.2	68
262	Capsaicin-induced corneal lesions in mice and the effects of chemical sympathectomy. Journal of Pharmacology and Experimental Therapeutics, 1987, 243, 690-5.	2.5	20
263	Biosynthesis and further transformations of leukotriene A4. Advances in Prostaglandin, Thromboxane, and Leukotriene Research, 1987, 17A, 64-8.	0.2	1
264	Corneal lesions induced by the systemic administration of capsaicin in neonatal mice and rats. Naunyn-Schmiedeberg's Archives of Pharmacology, 1984, 326, 347-351.	3.0	39
265	Prostaglandin Inactivation in Normal and Sensitized Guinea-pig Lung and its Inhibition by Indomethacin. Japanese Journal of Medicine, 1976, 15, 12-17.	0.1	3
266	Electron microscopic studies on mineral movement of calcifying process on the hard tissues. Japanese Journal of Oral Biology, 1972, 14, 560-570.	0.1	10